Available online at www.sciencedirect.com
SCIENCE DIRECT®
Journal of the European Ceramic Society 25 (2005) 1591–1595
www.elsevier.com/locate/jeurceramsoc

^{96}Zr diffusion in polycrystalline scandia stabilized zirconia

M.A. Taylor[a,1], M. Kilo[a,*], G. Borchardt[a], S. Weber[b], H. Scherrer[b]

[a] *TU Clausthal, Institut für Metallurgie, AG Thermochemie und Mikrokinetik, Robert-Koch-Str. 42, D-38678 Clausthal-Zellerfeld, Germany*
[b] *Ecole des Mines de Nancy, Laboratoire de Physique des Matériaux, Parc de Saurupt, F-54042 Nancy Cedex, France*

Received 27 March 2004; received in revised form 25 May 2004; accepted 31 May 2004
Available online 17 August 2004

Abstract

Diffusion of the stable tracer isotope ^{96}Zr in 12 mol% polycrystalline scandia stabilized zirconia was studied in air in the temperature range from 1200 to 1600 °C. Secondary ion mass spectroscopy (SIMS) was used to record the tracer diffusion profiles. The activation enthalpies for bulk and grain boundary diffusion were determined to be (5.0 ± 0.4) eV and (3.9 ± 0.5) eV, respectively, with the latter being six to seven orders in magnitude faster than the first. Using XRD, it was proved that the diffusion occurs only in the cubic phase.

Keywords: Diffusion; Surfaces; Grain boundaries; ZrO_2

1. Introduction

Pure zirconium dioxide (ZrO_2) has three polymorph phases: monoclinic (room temperature), tetragonal (above 1170 °C) and cubic phase (above 2370 °C). The addition of aliovalent ions to ZrO_2 fully or partially stabilizes the high temperature phases at low temperatures and creates anion vacancies resulting in an increased oxygen conductivity making the material useful as sensors and solid electrolytes in solid oxide fuel cells (SOFC). ZrO_2 stabilized with 10–12 mol% Sc_2O_3 (ScSZ) has the highest oxygen conductivity[1] of all zirconias doped with lower valent cation; its conductivity is about three times higher than that of Y_2O_3 stabilized zirconia (YSZ) with the same dopant level. Since the price of scandium dropped recently significantly, the system Sc_2O_3–ZrO_2 gained increased attraction for investigating its applicability in technological devices.

The phase diagram of the Sc_2O_3–ZrO_2 system is more complex than of other pseudo-binary M_2O_3–ZrO_2 systems. In contrast to other zirconia-based systems, in the scandia–zirconia system also the presence of rhombohedral phases are reported. In the concentration range where the highest oxygen conductivity is observed (10–12 mol% Sc_2O_3), the rhombohedral β-phase is stable at temperatures below 500 and 600 °C. Some authors indicated the occurrence of a loss of ionic conductivity in scandia stabilized zirconia (ScSZ) coinciding with the phase transition between the cubic and the β-phase.[2] The maximum of the phase transition between the β-phase and the cubic phase was determined to be at a stabiliser content of 12 mol% Sc_2O_3 and a temperature of 600 °C.[3–8] There is still controversy about the nature of the phase transition[1,5] and on hysteresis effects.[2,7,8]

Both for YSZ and ScSZ, the ionic conductivity decreases for long annealing times.[1] As the degradation process is directly related with the mobility of the cations in the lattice, the knowledge of diffusion data for the cations will allow a better understanding of the degradation process as well as of mechanical properties like the diffusion creep at high temperatures. Until now, there are no direct data available on cation diffusion in scandia stabilized zirconia in the literature. For ceramic scandia-stabilised zirconia, there is one old work on creep giving an activation enthalpy of 3.9 eV and a "creep" exponent of $n = 1.48$.[9]

* Corresponding author.
E-mail addresses: martin.kilo@tu-clausthal.de (M. Kilo), taylor@fisica.unlp.edu.ar (M.A. Taylor).
[1] On leave from the Physics Department, University of La Plata. IFLP CONICET, Argentina. Member of Carrera del investigador científico CONICET, Argentina.

0955-2219/$ – see front matter © 2004 Elsevier Ltd. All rights reserved.
doi:10.1016/j.jeurceramsoc.2004.05.020

In the present study, the diffusion of the rare stable isotope ^{96}Zr in ceramic ScSZ containing 12 mol% Sc_2O_3 was investigated using secondary ion mass spectroscopy (SIMS). From the depth profiles, both bulk diffusivities and grain boundary diffusivities could be determined.

2. Experimental

The polycrystalline ScSZ material (12 mol% Sc_2O_3 according to an X-ray fluorescence analysis) was purchased from KERAFOL in the form of thin foils (180 μm). The chemical composition of the powders used to produce the foils indicates that the accumulated impurity level of Fe_2O_3, CaO, SiO_2, etc. is less than 0.3%. The density (determined by the Archimedes method) was higher than 98% of the theoretical density. The foils were gas proof; no open porosity was found. The samples were cut, ground and polished down to 1 μm diamond grain size. XRD analysis indicated the presence of only beta phase.

A nitric solution of $^{96}ZrO_2/Sc_2O_3$ with the proper concentration of scandium was deposited on the polished surface and was allowed to dry at 50 °C in air giving a thin tracer layer enriched in ^{96}Zr of about 20 nm thickness. The layer could be considered to be homogeneous on comparing with the dimension of the investigated region. The coated samples were heated for 2 h at 800 °C before performing the diffusion anneals in order to decompose remaining nitrates. The samples were heated at 1600, 1500, 1468, 1378, 1286 and 1216 °C in air. The heating time was increased as the diffusion temperature was decreased.

After annealing, the changes in the crystallographic structure of the samples were investigated using X-ray diffraction (XRD) on a Siemens D5000 powder diffractometer (Co Kα radiation, step width of 0.02°, fixed time of 5 s). The region of 55–65°, where the most noticeable differences between the cubic and the β-phase occur, was used to identify the two phases. The thermal stabilities of the observed phases were investigated with high temperature X-ray diffraction between room temperature and 1200 °C.

Stability of grain size was followed using SEM. Since in previous experiments, grain growth was observed at higher temperatures (>1500 °C) during the diffusion anneal experiments, the samples diffused at higher temperature were preheated at 1600 °C for 17 h to achieve stable grains size.

SIMS experiments were performed using a VG-SIMS-Lab at the Ecole des Mines in Nancy, France. An Ar^+ primary ion beam (8 keV, 150 nA) was scanned over an area of 300 μm × 300 μm. Singly charged positive secondary ions were detected. An electronic gating of 30% in each direction was applied to reduce crater edge effects. The depth of the crater, measured using a profilometer, was used to convert sputter time into depth. The depth inaccuracy resulting from the roughness of the crater bottom was in no case more than 10%.

Diffusional profiles were determined by measuring the signal intensities of six isotopes, ^{46}Sc, ^{90}Zr, ^{91}Zr, ^{92}Zr, ^{94}Zr, ^{96}Zr, on sputtering. As the analysis area (approximately 100 μm × 100 μm) was large compared to the grain size (approximately 10–30 μm) these intensities were proportional to the mean concentration $\bar{c}$ of the isotopes monitored at a given depth.

Bulk diffusivities D were calculated from the experimental results on fitting the following solution (Eq. (1)) of Fick's second law to the "bulk part" of the tracer isotope concentration profile, i.e. the part of the depth profile, which is close to the surface:[10]

$$\bar{c}(z,t) = \frac{M}{(\pi Dt)^{1/2}} \exp\left(-\frac{z^2}{4Dt}\right) \quad (1)$$

where, M is the quantity of diffusant per unit area at $z = 0$, z is the depth coordinate and t is the diffusion time.

The grain boundary diffusivity D_{GB} was determined according to Suzuoka's theory using the following equation:[11]

$$D_{GB}\delta = 1.308\left(\frac{D}{t}\right)^{1/2}\left[-\frac{\partial \ln \bar{c}}{\partial z^{6/5}}\right]^{-5/3} \quad (2)$$

where, δ is the grain boundary thickness, taken to be 10 Å.

Table 1 gives an overview over the characteristic parameters, which define the diffusion regime (in the so-called Isolated Grain Boundary Model) and the obtained diffusion coefficients. We applied Eq. (2) for the calculation of the grain boundary diffusivity from the tail of the profile, which means that grain boundary transport occurred in the so called B regime ($10\delta < (Dt)^{1/2} < d/10$), where d is the grain size.

Table 1
Experimental conditions and results of the diffusion experiments

T (°C)	t (h)	d (μm)	D_{bulk} (cm^2 s^{-1})	$(Dt)^{1/2}$ (10^{-5} cm)	$d/10$ (10^{-5} cm)	D_{GB} (cm^2 s^{-1})
1216	498	8	9.9×10^{-17}	1.33	8	4.5×10^{-10}
						8.2×10^{-10}
1286	223	10	2.0×10^{-16}	1.26	10	3.0×10^{-9}
1378	63.5	10	2.8×10^{-15}	2.54	10	4.8×10^{-8}
			8.1×10^{-15}			8.9×10^{-9}
1468	24.5	12	1.1×10^{-14}	5.35	12	1.2×10^{-7}
1500	20	30	$2.7 \times 10-^{14}$	4.45	30	2.8×10^{-8}
1600	1.93	30	3.8×10^{-13}	5.06	30	4.5×10^{-7}

The grain width δ was assumed to be 10^{-7} cm.

3. Results and discussion

Fig. 1 shows the SIMS profile obtained on a sample annealed at 1378 °C for 63.5 h. A typical ^{96}Zr diffusion profile is shown with the part dominated by the bulk diffusion close to the surface (region A) and the part dominated by grain boundary diffusion at higher sample depth values (region B). Solid lines are the fitted curves using Eqs. (1) and (2), respectively. For region B it is possible to get a reliable fit according to Eq. (2) despite the fact that the natural abundance of the stable isotope ^{96}Zr (2.78%) is rather high and therefore the dynamic range of the tail is relatively low. Close to the surface, the signal intensity of ^{96}Zr is slightly reduced due to the establishment of the sputter equilibrium at the beginning of the sputter process.

XRD experiments performed at room temperature before and after the diffusion experiments indicated that the while the samples originally all were in the β-phase, the β-phase was observed for the samples treated at 1215, 1286 and 1378 °C and the cubic phase for the sample heated above 1468 °C (Fig. 2). High temperature XRD experiments performed up to 1400 °C indicate that all samples transform to the cubic below the temperatures were the diffusion experiments were performed. This means that in all cases the diffusion takes place in the cubic phase. On cooling the samples, the retransformation from the cubic to the β-phase was not complete in all cases for kinetic reasons.

The diffusion coefficients, calculated for each regime from the experimental data using Eqs. (1) and (2), are shown in Fig. 3 as a function of temperature in an Arrhenius plot.

The activation enthalpies obtained from fitting the experimental results were $\Delta H_{Bulk} = (5.0 \pm 0.4)$ eV for bulk diffusion and $\Delta H_{GB} = (3.9 \pm 0.5)$ eV for grain boundary diffusion, with preexponential factors of 5.1 and 1.5×10^4 cm^2 s^{-1}. The value for the activation enthalpy of grain boundary diffusion is in excellent agreement with the old creep data reported by Evans.[9]

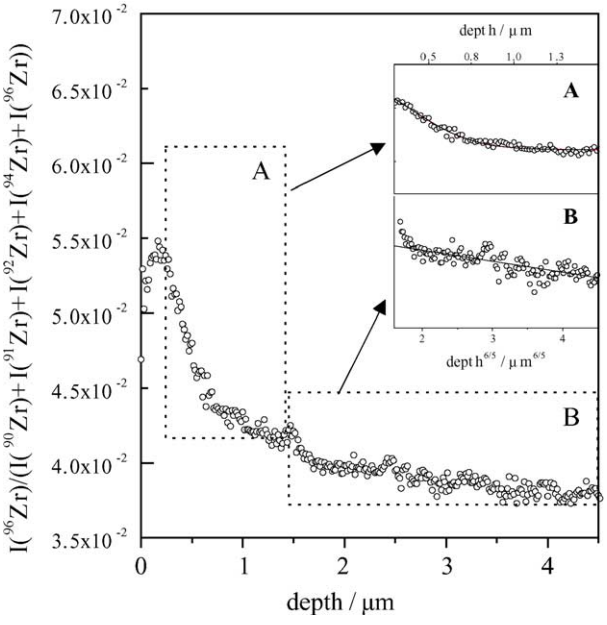

Fig. 1. ^{96}Zr depth profile for a sample annealed at 1378 °C for 63.5 h. Full lines are the results of fitting the bulk and the grain boundary diffusion parts according to Eqs. (1) and (2) (see inserts).

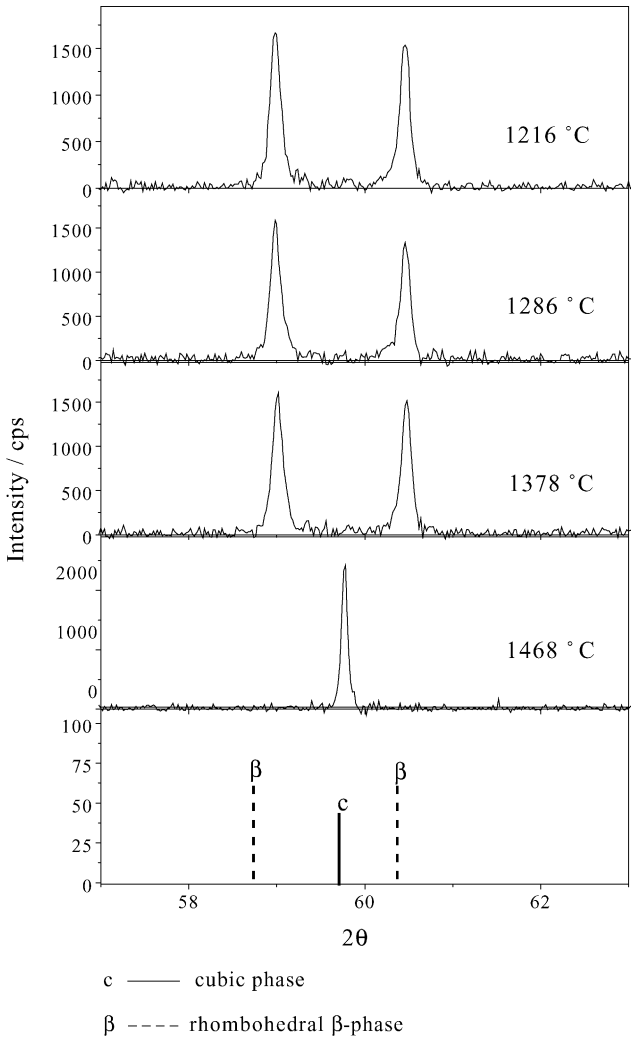

Fig. 2. X-ray diffraction patterns of selected diffusion annealed samples. Shown are also the 2θ values indicative for the rhombohedral and cubic phases.

On comparing the diffusivities obtained for the ScSZ material with earlier results on CSZ (11 mol%)[12] and YSZ (10 mol%)[13] with similar dopant content, it is found that in the whole investigated temperature range, the zirconium diffusivity in ScSZ is higher than in the other zirconia materials. This higher diffusion coefficient could be the cause for the easier ordering effects observed in the ScSZ as to the other stabilized zirconia (see Fig. 4).

Kowalski et al.[14,15] investigated the diffusion of Ca and Ti in YSZ. These authors argue that for ions with ionic radii close to the ionic radius of Zr, the ratio q between the activation enthalpy for grain boundary diffusion and the activation enthalpy for bulk diffusion ($q = \Delta H_{GB}/\Delta H_{Bulk}$) is almost the same and less than 1 ($q = 0.67 \pm 0.12$ for Ti and $q = 1.10$

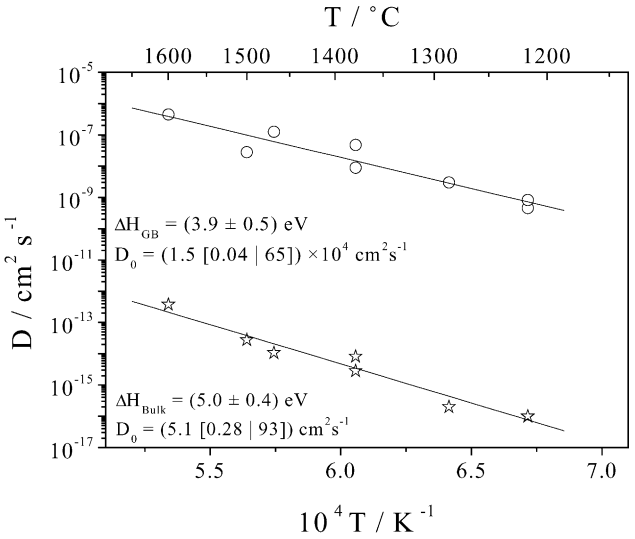

Fig. 3. Temperature dependency of ^{96}Zr tracer diffusivities. Symbols correspond to bulk diffusion (☆), and grain boundary diffusion (○), respectively.

± 0.22 for Ca). More recently, Bak et al.[16] found on investigating the Mg diffusion in YSZ that the activation enthalpies for the bulk diffusion and grain boundary diffusion are 4.05 and 1.26 eV, respectively, giving a ratio of $q = 0.31$. Our result for ^{96}Zr tracer diffusion gives an enthalpy ratio of $q = 0.76 \pm 0.16$, which is lower than 1 within experimental error. Fig. 5 gives an overview of known q values as a function of the diffusant radius r.[17] As can be seen, no simple linear correlation can be established between $\Delta H_{GB}/\Delta H_{Bulk}$ and the ionic radius of the diffusing species, except that mostly all q values are lower than one with the exception of the Mn values. Regarding this atom, some studies indicated that the oxidation state of manganese in YSZ is a mixture of 2+ and 3+[18] implying a change on the ionic radius.

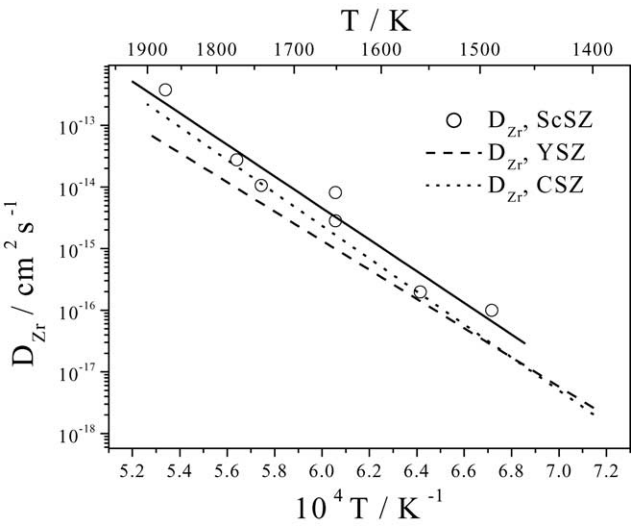

Fig. 4. Comparison of the Zr diffusivities in 11 mol% YSZ (dashed line), 11 mol% CSZ (dotted line) and ScSZ (points and solid line).

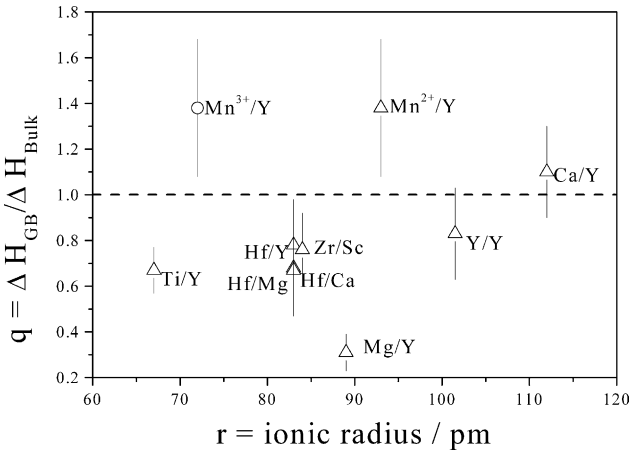

Fig. 5. Activation enthalpy ratio q of grain boundary diffusion and bulk diffusion as a function of the ionic radius of the diffusant. For the couples diffusant/stabilizer element the following data were used, with Y corresponding to YSZ, Ca to CSZ and Mg to MgSZ: Mn^{2+}/Y (Mn^{3+}/Y): reference 18; Ti/Y: reference 15; Ca/Y: reference 14; Hf/Y: reference 15 and references therein; Hf/Ca: reference 15 and references therein; Hf/Mg: reference 15 and references therein; Y/Y: reference 22; Zr/Sc: this work; Mg/Y: reference 16. The ionic radii were taken from reference 16 for a coordination number (CN) of 8, except for Mn^{3+} where only CN = 6 exists.[22]

Furthermore, Kowalski et al. pointed out that differences in the composition and/or structure of the grain boundaries could influence the cation transport across them making this process dependent on the composition of the individual samples. The observed differences for the q value for Mn diffusion could be either due to the change in the valence state or due to inhomogeneities in the grain boundary of the manganese-containing samples.

The preexponential factor in the Arrhenius expression for the diffusivity can be related to the activation entropy of diffusion as follows:

$$D_0 = \lambda^2 \eta \exp\left(\frac{S_f + S_m}{k_B}\right) \quad (3)$$

where, λ is the jump distance, η is the vibration frequency and S_f and S_m are the formation and migration entropies for cation vacancies, respectively. Taking $\lambda = 0.392$ nm in ZrO_2 and $\eta = 10^{13}\ s^{-1}$,[19] an entropy factor of 6 k_B can be calculated from the bulk experimental value for D_0 for the sum of the two entropy contributions. Comparing this value with the available literature data,[20] a zirconium migration via free vacancies can be assumed as was also proposed earlier for the similar YSZ system.[21]

4. Conclusions

- The zirconium bulk and grain boundary diffusivities in ScSZ containing 12 mol% Sc_2O_3 were successfully determined using the stable isotope ^{96}Zr. It was shown for the first time that also with the not extremely rare stable

isotope ^{96}Zr (2.78% abundance), grain boundary diffusion coefficients can be obtained. The bulk diffusion is by six to seven orders of magnitude slower than the grain boundary diffusion.

- Activation enthalpies for bulk diffusion and for grain boundary diffusion were determined to be (5.0 ± 0.4) eV and (3.9 ± 0.5) eV, respectively.
- The entropy derived from the D_0 value of the bulk diffusion (6 k_B) suggested that the diffusion process proceeded via free vacancies as in the YSZ system.
- The diffusion of zirconium in ScSZ is higher than in other stabilised zirconias containing the same amount of stabiliser.
- The activation enthalpy for zirconium grain boundary diffusion is lower than for zirconium bulk diffusion, which is in-line with previous investigations.

Acknowledgements

The Deutsche Forschungsgemeinschaft supported this work. One of the authors (M.A.T.) gratefully acknowledges partial financial support by CONICET, Argentina.

References

1. Kharton, V. V., Naumovich, E. N. and Vecher, A. A., Research on the electrochemistry of oxygen ion conductors in the former Soviet Union. I. ZrO_2-based ceramic materials. *J. Solid State Electrochem.*, 1999, **3**, 61–81 and references therein.
2. Ishii, T., Iwata, T. and Tajima, Y., Structure phase transition and ion conductivity in $0.88ZrO_2$–$0.12Sc_2O_3$. *Solid State Ionics*, 1992, **57**, 153–157.
3. Sheu, T. S., Xu, J. and Tien, T. Y., Phase relationships in the ZrO_2–Sc_2O_3 and ZrO_2–In_2O_3 systems. *J. Am. Ceram. Soc.*, 1993, **76**, 27–32.
4. Hirano, M., Watanabe, S., Kato, E., Mizutani, Y., Kawai, M. and Nakamura, Y., High electrical conductivity and high fracture strength of Sc_2O_3-doped zirconia ceramics with submicrometer grains. *J. Am. Ceram. Soc.*, 1999, **82**, 861–864.
5. Haering, C., Roosen, A. and Schichl, H., Alterungsphänomene von Yttriumoxid- und Scandiumoxid-dotiertem Zirkoniumdioxid nach Auslagerungen bei 1000 °C. Preprint of a manuscript, presented at Werkstoffwoche München 12–15 Okt., 1998.
6. Sakuma, T. and Suto, H., The cubic-to-β martensitic transformation. *J. Mater. Sci.*, 1986, **21**, 4359–4365.
7. Lefevre, J., Phases of fluorite-type in the zirconia-based system. *Ann. Chim. (Paris)*, 1963, **8**, 117–149.
8. Wurst, K., Schweda, E., Bevan, D. J. M., Mohyla, J., Wallwork, K. S. and Hofmann, M., Single-crystal structure determination of $Zr_{50}Sc_{12}O_{118}$. *Eur. J. Solid State Inorg. Chem.*, 2003, **5**, 1491–1498.
9. Evans, P. E., Creep in yttria- and scandia-stabilized zirconia. *J. Am. Ceram. Soc.*, 1970, **53**, 365–369.
10. Crank, J., *The Mathematics Of Diffusion*. Oxford University Press, Oxford, 1975.
11. Kaur, I., Mishin, Y. and Gust, W., *Fundamentals of Grain and Interphase Boundary Diffusion* (*3rd ed.*). John Wiley and Sons, New York, 1995 (Chapter 2).
12. Kilo, M., Borchardt, G., Weber, S., Scherrer, S., Tinschert, K., Lesage, B. *et al.*, Cation diffusion in calcia stabilized zirconia (CSZ). *Rad. Eff. Defects*, 1999, **151**, 29–33.
13. Kilo, M., Fundenberger, C., Borchardt, G., Herzog, R., Lakki, A., Weller, M. *et al.*, Oxygen and host transport in Yttria stabilized zirconia. *Ceram. Trans.*, 1997, **109**, 133–142.
14. Kowalski, K., Bernasik, A. and Sadowski, A., Diffusion of calcium in yttria stabilized zirconia ceramics. *J. Eur. Ceram. Soc.*, 2000, **20**, 2095–2100.
15. Kowalski, K., Bernasik, A. and Sadowski, A., Bulk and grain boundary diffusion of titanium in yttria stabilized zirconia. *J. Eur. Ceram. Soc.*, 2000, **20**, 951–958.
16. Bak, T., Nowotny, J., Prince, K., Rekas, M. and Sorrell, C. C., Grain boundary diffusion of magnesium in zirconia. *J. Am. Ceram. Soc.*, 2002, **85**, 2244–2250.
17. Shannon, R. D. and Prewitt, C. T., Effective ionic radii in oxides and fluorides. *Acta Cryst.*, 1969, **B25**, 925–946.
18. Waller, D., Sirman, J. D. and Kilner, J. A., Manganese diffusion in single crystal and polycrystalline yttria stabilized zirconia. *Electrochem. Proc.*, 1997, **97**, 1140–1149.
19. Chien, F. R. and Heuer, A. H., Lattice diffusion kinetics in Y_2O_3-stabilized cubic ZrO_2 single crystals: a dislocation loop annealing study. *Philos. Mag.*, 1996, **73**, 681–697.
20. Phillibert, J., *Atom Movements: Diffusion and Mass Transport in Solids*. Editions de Physique, Les Ulis, 1991.
21. Kilo, M., Borchardt, G., Lesage, B., Kaïtasov, Weber, S. and Scherrer, S., Cation transport in yttria stabilized cubic zirconia: ^{96}Zr tracer diffusion in $(Zr_xY_{1-x})O_{2-x/2}$ single crystals with $0.15 \leq x \leq 0.48$. *J. Eur. Ceram. Soc.*, 2000, **20**, 2069–2077.
22. Kilo, M., Taylor, M. A., Argirusis, C., Borchardt, G., Lesage, B., Weber, S. *et al.*, Cation self diffusion of ^{44}Ca, ^{88}Y and ^{96}Zr in single crystalline calcia- and yttria-doped zirconia. *J. Appl. Phys.*, 2003, **94**, 7547–7552.